Protein Expression and Purification 166 (2020) 105522

Contents lists available at ScienceDirect

Protein Expression and Purification

journal homepage: www.elsevier.com/locate/yprep

Strategies for successful isolation of a eukaryotic transporter

Savvas Saouros[a], Cristina Cecchetti[a], Alex Jones[b], Alexander D. Cameron[b], Bernadette Byrne[a,*]

[a] Department of Life Sciences, Imperial College London, Exhibition Road, London, SW7 2AZ, UK
[b] School of Life Sciences, University of Warwick, Gibbet Hill Road, Coventry, CV4 7AL, UK

ARTICLE INFO

Keywords:
BOR protein
Transporter
Truncation
Purification
Detergent
Neopentyl glycol
Stability
Oligomeric state

ABSTRACT

The isolation of integral membrane proteins for structural analysis remains challenging and this is particularly the case for eukaryotic membrane proteins. Here we describe our efforts to isolate OsBOR3, a boron transporter from *Oryza sativa*. OsBOR3 was expressed as both full length and a C-terminally truncated form lacking residues 643–672 ($OsBOR3_{\Delta 1\text{-}642}$). While both express well as C-terminal GFP fusion proteins in *Saccharomyces cerevisiae*, the full length protein isolates poorly in the detergent dodecyl-β-*d*-maltoside (DDM). The $OsBOR3_{\Delta 1\text{-}642}$ isolated in DDM in large quantities but was contaminated with GFP tagged protein, indicated incomplete protease removal of the tag. Addition of the reducing agent dithiothreitol (DTT) had no effect on isolation. Detergent screening indicated that the neopentyl glycol detergents, LMNG, UDMNG and DMNG conferred greater stability on the $OsBOR3_{\Delta 1\text{-}642}$ than DDM. Isolation of $OsBOR3_{\Delta 1\text{-}642}$ in LMNG both in the presence and absence of DTT produced large quantities of protein but contaminated with GFP tagged protein. Isolation of $OsBOR3_{\Delta 1\text{-}642}$ in DMNG + DTT resulted in protein sample that does not contain any detectable GFP but elutes at a higher retention volume than that seen for protein isolated in either DDM or LMNG. Mass spectrometry confirmed that the LMNG and DMNG purified protein is $OsBOR3_{\Delta 1\text{-}642}$ indicating that the DMNG isolated protein is monomer compared to the dimer isolated using LMNG. This was further supported by single particle electron microscopic analysis revealing that the DMNG protein particles are roughly half the size of the LMNG protein particles.

1. Introduction

Integral membrane proteins have roles in a range of essential cellular functions including respiration, photosynthesis, membrane transport and mediation of cellular responses to environmental change. Given their crucial importance, they represent the targets for > 50% of currently available drugs [1]. The last 15 years have seen a significant increase in our understanding of their mechanism of action, largely due to advancements in technology that has allowed the determination of many new high resolution structures [2]. Despite this substantial progress, the isolation of membrane proteins for structural studies remains challenging [3], due to the highly hydrophobic nature of these molecules. To date most structures have been solved by first extracting the protein from the membrane [4], even if, ultimately, they are reconstituted back into a lipid environment for further analysis.

The standard methodology for extraction and solubilisation of membrane proteins in an aqueous based solution involves the addition of detergents. The latter are amphiphilic molecules that possess both hydrophobic and hydrophilic properties and share this characteristic with the membrane proteins and the membrane lipid bilayer [4]. For this reason, detergent micelles disrupt the interactions between the membrane protein and the lipid environment and encapsulate the protein molecules forming a protein detergent complex [5]. A suitable detergent for structural studies extracts the protein from the membrane with high efficiency whilst retaining the tertiary/quaternary structure of the protein. A relatively small number of detergents including dodecyl-β-*d*-maltoside (DDM) and decyl-β-*d*-maltoside (DM) are typically used for initial membrane protein extraction and solubilisation [6] with these detergents also contributing to a substantial number of membrane protein structures [7,8]. Although it should be noted that the detergent used for extraction and isolation may be exchanged for another prior to crystallisation trials or the detergent used for solubilisation and purification can be used in combination with another detergent in the form of mixed micelles [8]. However, many membrane proteins are not stable in even these relatively mild detergents [9]. The standard detergents tend to have similar overall architecture which is likely to contribute to their limited application to the wide variety of integral membrane proteins structures [9].

Given that many membrane proteins are not stable even in relative mild detergents [9], substantial efforts have been made over the last decade to expand the range of detergents suitable for membrane protein manipulation (for example [10–12]). Of particular relevance for

* Corresponding author. Department of Life Sciences, Imperial College London, Exhibition Road, SW7 2AZ, UK.
E-mail address: b.byrne@imperial.ac.uk (B. Byrne).

https://doi.org/10.1016/j.pep.2019.105522
Received 9 August 2019; Received in revised form 18 October 2019; Accepted 20 October 2019
Available online 23 October 2019
1046-5928/

Table 1
Primer sequences.

Construct	Forward primer	Reverse primer
OsBOR3	5′ACCCCGGATTCTAGAACTAGTGGATCCCCCATGGAACTACTAAAGATTCCCTTTAAGGGTGTCGTC3′	5′AAATTGACCTTGAAAATATAAATTTTCCCGCACTGGACCAGTTTTCTGTATCTCCACACCTGGG3′
$OsBOR3_{\Delta 1\text{-}642}$	As above	5′AAATTGACCTTGAAAATATAAATTTTCCCCTCTGTGCTTTAGCTCTCCACGGTTAGTTGTCAGCTC3′

membrane protein manipulation are the maltose neopentyl glycols (MNGs) and glucose neopentyl glycols (GNGs) [13,14], which have been shown to be suitable for both extraction and stabilisation of membrane proteins and have contributed to the structure determination of approximately 30 novel membrane protein structures (see Ref. [15] and references cited therein). These include ATPases, the $GABA_A$ ligand gated ion channel, and the tight junction, claudin, as well as a number of GPCRs. The MNGs and GNGs induce greater stability to associated membrane proteins compared to standard detergents, suggested to be the result of the incorporation of a quaternary C atom into their chemical architecture. The increased stability of the proteins is predicted to be due to the greater stability of the detergent micelles [13,14].

Different approaches include the amphipols [16] and peptidiscs [17], which are not suitable for extraction. The amphipols, however, have been successfully used to stabilize purified membrane protein for structural studies by Cryo-EM (for example [18,19], following detergent exchange. Membrane proteins can also be reconstituted in nanodiscs, a discoidal lipid bilayer held together by two helical scaffold proteins, after the solubilisation step. Despite still requiring the solubilisation step, this method has the advantage of reducing the amount of detergent used and ultimately results in membrane proteins in a more native lipid environment which can be studied using a variety of techniques [20].

A set of novel agents are based on the styrene maleic acid (SMA) copolymer architecture which have the ability of intercalating between the acyl chains of the membrane bilayer and extracting both the integral membrane protein and the lipids. The SMA lipid particles (SMALPs) therefore result in a central lipid bilayer surrounded by the polymer [21–24].

Boron (B) is an essential plant nutrient with a key role in the generation of ester cross-linked rhamnogalacturonan II through the formation of apisoyl dimers, essential for structure and function of the extracellular matrix [25,26]. B deficiency and toxicity are major barriers to efficient crop growth in many parts of the world. B uptake, efflux and distribution are mediated by a complex system of integral membrane channels and transporters. The borate transporters have roles in both active transport of B for xylem loading and efflux of B into the soil when intracellular B concentrations reach toxic levels [27,28]. Despite the importance of these proteins in the effective delivery of B to developing and growing plant tissues, remarkably little is known about their mechanism of action. Most of the research carried out on BOR proteins has focused on the *Arabidopsis thaliana* BOR1, a 14 transmembrane domain protein, which is expressed in the root endodermis. Indeed, there is a low resolution X-ray crystallographic structure of AtBOR1 (PDB: 5L25) [29], although this lacks virtually all the soluble loop regions and many mechanistic details about B transport remain to be understood. Additional clues on the structure and mechanism of action of BOR proteins come from structures of the BOR homologues (AE1 (PDB: 4YZF) [30] and NCBe1 (PDB: 6CAA) [31]) as well as the structurally related nucleobase ascorbate transporters, (UapA (PDB 5I6C) [32] and UraA (PDB: 5XLS) [33].

Several AtBOR1 homologues exist in rice (*Oryza sativa*) and here we describe efforts to isolate the OsBOR3 homologue (shares 57.8% sequence identity with AtBOR1) both as full length and C-terminally truncated versions in an effort to obtain sufficiently pure and stable protein for structural studies. We purified the two different forms of OsBOR3 and found that isolation of the proteins was highly sensitive to the detergent used. The quality of the preparations increased when we used either LMNG or DMNG, compared to DDM.

2. Methods

2.1. Construct generation

The open reading frame of OsBOR3 (Accession code: AY339063)

was obtained from the Rice Genome Resource Centre, Tsukuba, Japan). The full-length OsBOR3 and C-terminally truncated versions, $OsBOR3_{\Delta 1\text{-}642}$ (missing amino acid residues 643–672) were expressed as C-terminal yeast enhanced GFP fusion proteins using the *S. cerevisiae* expression vector pDDGFP2 and the FGY217 protease deficient strain [34] as previously described [32,35] using the oligonucleotide primers detailed in Table 1. These primers contain homologous recombination domains allowing direct insertion of the gene into the expression vector.

2.2. Small scale expression and membrane preparation

Expression and purification were carried out based on previously described methods [36,37]. For expression of the individual constructs, single colonies from yeast transformations were incubated overnight in 5 mL of -URA media supplemented with 2% glucose at 30 °C with 300 rpm shaking. The cells were diluted to an OD_{600} of 0.12 in 50 mL -URA media supplemented with 0.1% glucose and incubated at 30 °C and 300 rpm shaking until an OD_{600} of 0.6 was reached. Protein expression was induced by adding 25% galactose in -URA media to a final concentration of 2%. Cells were incubated for a further 22 h. Cells were pelleted by centrifugation at 3000*g* for 5 min at 4 °C and resuspended in 1 mL CRB (50 mM Tris (pH 7.5), 1 mM EDTA, 0.6 M sorbitol) supplemented with cOmplete™ EDTA free protease inhibitor tablets (Roche). 200 µL resuspended cells were analysed by a SpectraMax M2e fluorometer (Molecular Devices) using an excitation wavelength of 488 nm and an emission wavelength of 512 nm to assess the degree of protein expression by measuring the levels of GFP fluorescence in the sample. Glycerol stocks of the samples with the highest protein expression were used for large scale protein expression. The cells were lysed using 0.5 mm glass beads at 400 µL mL^{-1} and a FastPrep_24 5G (MP) with pulses for 20 s at a speed of 6 m/sec, repeated 6 times. The cells were kept on ice for 2 min between each round of lysis. Intact cells were pelleted by centrifugation at 14000*g* for 30 s. The supernatant was harvested and subjected to centrifugation at 22000*g* for 1 h at 4 °C to pellet membranes which were resuspended in 150 µL MRB (20 mM Tris (pH 7.5), 0.3 M sucrose, 0.1 mM calcium chloride). Membranes were flash-frozen in liquid nitrogen and stored at −80 °C. The membranes obtained were used to assess expression of the different constructs and for FSEC analysis.

2.3. FSEC analysis

Aliquots of membranes (150 µL) prepared from yeast cell cultures overexpressing OsBOR3 were added to 1 mL solubilisation buffer (1x PBS (pH 7.5), 100 mM NaCl, 1% DDM (w/v)) supplemented with cOmplete™ EDTA free protease inhibitor tablets (Roche). Membranes were solubilised by gentle mixing at 4 °C on an orbital shaker for 1 h. Insoluble membranes were pelleted by centrifugation for 1 h at 15000 *g* at 4 °C. 500 µL supernatant was loaded onto a Superose 6 10/300 gel filtration column equilibrated with FSEC buffer (20 mM Tris (pH 7.5), 150 mM NaCl, 0.03% DDM (v/v)) and fractions were collected on a 96 well optical bottom plate. Fluorescence of the individual fractions was measured using a SpectraMax M2e fluorometer (Molecular Devices) ($\lambda_{excitation}$ = 488 nm, $\lambda_{emission}$ = 512 nm).

2.4. Large scale OsBOR3 purification

For large scale production of the OsBOR3 proteins, membranes were prepared from a 12 L *S. cerevisiae* culture using a cell disruptor (Constant Systems) and differential centrifugation to remove unbroken cells and then harvest the membranes. The membranes were solubilised for 1 h at 4 °C with stirring in a total of 150 mL membrane solubilisation buffer (1x PBS (pH 7.5), 100 mM NaCl, 10% glycerol (v/v), 1% n-dodecyl-β-D-maltoside (DDM) or 1% DMNG or 1% LMNG (w/v)) supplemented with protease inhibitor tablets (Roche). Remaining insoluble material was pelleted by centrifugation at 100000*g* for 45 min. The supernatant was loaded onto a 5 mL His-trap column (G.E. Biosciences) equilibrated with affinity buffer (1x PBS (pH 7.5), 100 mM NaCl, 10 mM imidazole, 10% glycerol, 0.03% DDM (v/v)). The column was washed three times with 50 mL affinity buffer supplemented with 30 mM, then 50 mM, and finally 70 mM imidazole. His-tagged OsBOR3 was eluted from the column with 50 mL elution buffer (1x PBS (pH 7.5), 100 mM NaCl, 350 mM imidazole, 10% glycerol, 0.03% DDM (v/v)). Eluted protein was diluted into a total of 100 mL SEC buffer (20 mM Tris (pH 7.5), 150 mM NaCl, 2 x DDM, CxEx or Triton X-100). The His-tag was removed by incubating OsBOR3 with TEV protease at a ratio of 1:1 overnight. The protein sample was filtered using a 0.22 µm filter (Millex) and loaded onto a 5 mL His-trap column (G.E. Biosciences) equilibrated with SEC buffer supplemented with 10 mM imidazole. Non-His-tagged OsBOR3 was recovered in the initial column flow through and via washing the column with 25 mL SEC buffer supplemented with 10 mM imidazole. OsBOR3 was concentrated to 500 µL using a 100 kDa MWCO filter (Millipore). Aggregated material was removed by centrifugation at 22000*g* for 10 min at 4 °C. OsBOR3 was loaded onto a Superdex 200 10/300 gel filtration column pre-equilibrated with SEC buffer. Elution fractions were analysed by SDS-PAGE using precast Novex™ WedgeWell™ 10% Tris-Glycine Gel (Invitrogen). Protein bands were stained using Coomassie Instant Blue (Expedeon) and visualised using a BIO-RAD ChemiDoc MP Imaging System. In gel fluorescence was visualised using a Fujifilm LAS-3000 imager. 2 mM DTT was added in all buffers in the protein purifications were DTT was used.

2.5. Thermal denaturation analysis

Thermal denaturation assays were carried out to assess the stability of the OsBOR3 in a range of different detergents typically used for preparation of protein for native MS analysis. In each case 1 µL of pure OsBOR3 at ~10 mg/mL and in buffer containing 2 x CMC DDM was diluted into 150 µL of thermal denaturation buffer (150 µL 20 mM Tris (pH 7.5), 150 mM NaCl, 2x CMC detergent of interest) in a 96 well clear bottom plate. The detergents tested were DDM, n-decyl-β-D-maltoside (DM), n-nonyl-β-D-maltoside (NM), lauryl maltose neopentyl glycol (LMNG), undecyl maltose neopentyl glycol (UDMNG) decyl maltose neopentyl glycol (DMNG) and octyl glucose neopentyl glycol (OGNG). In the dark, 3 µL (40 µg/mL) 7-diethylamino-3-(4′-maleimidylphenyl)-4-methylcoumarin (CPM) dye diluted in thermal denaturation buffer (Invitrogen) was added to each well. The plate was incubated at 40 °C and fluorescence measured every 5 min for 2 h using a SpectraMax plate reader (Molecular Devices) ($\lambda_{excitation}$ = 387 nm, $\lambda_{emission}$ = 463 nm). The raw fluorescence readings were normalized to the most unstable condition in order to calculate the percentage of relative unfolded protein. The data were fitted to a single exponential decay curve using GraphPad Prism 6.

2.6. Long term stability analysis

Aliquots of pure OsBOR3 protein at 10 mg/mL were stored at either 4 °C or 20 °C. On day 1, 2 and 4 1 µl protein was removed from the individual aliquots, mixed 1:1 with NOVEX™ Tris-Glycine SDS Sample Buffer, 2X (Invitrogen) and stored at −20 °C until further use. After 4 days all the samples were separated on SDS-PAGE gels and the protein bands visualised using Coomassie Blue gel Stain.

2.7. Negative stain EM

Negative stain EM was used to assess sample quality during purification. 2.5 µL of $OsBOR3_{\Delta 1\text{-}642}$ at a concentration of 0.01 mg/mL was applied to glow-discharged carbon-coated copper grids (400 mesh) and stained with 2% uranyl acetate. Data were collected on a 120 keV Tecnai T12 microscope.

Table 2
Summary data for the different constructs and detergents.

	Construct	
	WT OsBOR3	$OsBOR3_{\Delta1\text{-}642}$
Expression (mg/L)	0.600	0.950
Solubilisation efficiency in DDM (%)	80	85
Purification yield in DDM (mg/L)	0.015	0.100
Purification yield in DDM + DTT (mg/L)	nd	0.100
Solubilisation efficiency in LMNG (%)	nd	80
Purification yield in LMNG (mg/L)	nd	0.125
Purification yield in LMNG + DTT (mg/L)	nd	0.125
Solubilisation efficiency in DMNG (%)	nd	80
Purification yield in DMNG + DTT (mg/L)	nd	0.125

Nd = not determined.

3. Results and discussion

3.1. Expression of the different OsBOR3 constructs and isolation of the protein in DDM

Both the WT and $OsBOR3_{\Delta1\text{-}642}$ constructs expressed well, to levels of 0.6 mg/L and 0.95 mg/L respectively. A summary of expression levels, solubilisation efficiencies and purification yields is given in Table 2.

The first protein to be purified was WT OsBOR3 in DDM. The SEC trace indicated a very heterogeneous sample with multiple overlapping peaks (Fig. 1A). The SDS-PAGE analysis of some of these fractions indicated a single prominent band at ~30 kDa (Fig. 1B) present in all samples. It is possible that a number of different aggregated forms of the OsBOR3 are isolating on the SEC column that dissociate into a single species on the gel. The high heterogeneity and very low overall yield of full length OsBOR3 (0.015 mg/L) meant that this construct was not explored further.

We then attempted isolation of $OsBOR3_{\Delta1\text{-}642}$ in DDM and achieved much better results. The SEC trace gave a single peak with a retention volume of about 11 mls (Fig. 1C) and the fractions tested yielded one prominent band of approximately 80 kDa on an SDS-PAGE (Fig. 1D-, upper panel) although some aggregated material was observable in the wells. Given the fact that membrane proteins often appear smaller than they are on SDS-PAGE gels [38] and the expectation that OsBOR3 is likely to be a dimer [29,30,39] it wasn't clear what the bands we were seeing corresponded to. The yield of $OsBOR3_{\Delta1\text{-}642}$ was ~0.100 mg/L, and although this together with the homogeneity of the sample represented a significant improvement compared to the full length OsBOR3, the material was contaminated with GFP (Fig. 1D, lower panel). Indeed, following concentration to 10 mg/ml the protein sample was visibly green and it is possible that the ~80 kDa band we see which on the Coomassie stain gel is the $OsBOR3_{\Delta1\text{-}642}$ + GFP which is also clearly visible on the in-gel fluorescence.

Despite a clear monodispersed peak for the of $OsBOR3_{\Delta1\text{-}642}$ the gel image indicated the sample was markedly heterogeneous. This might be

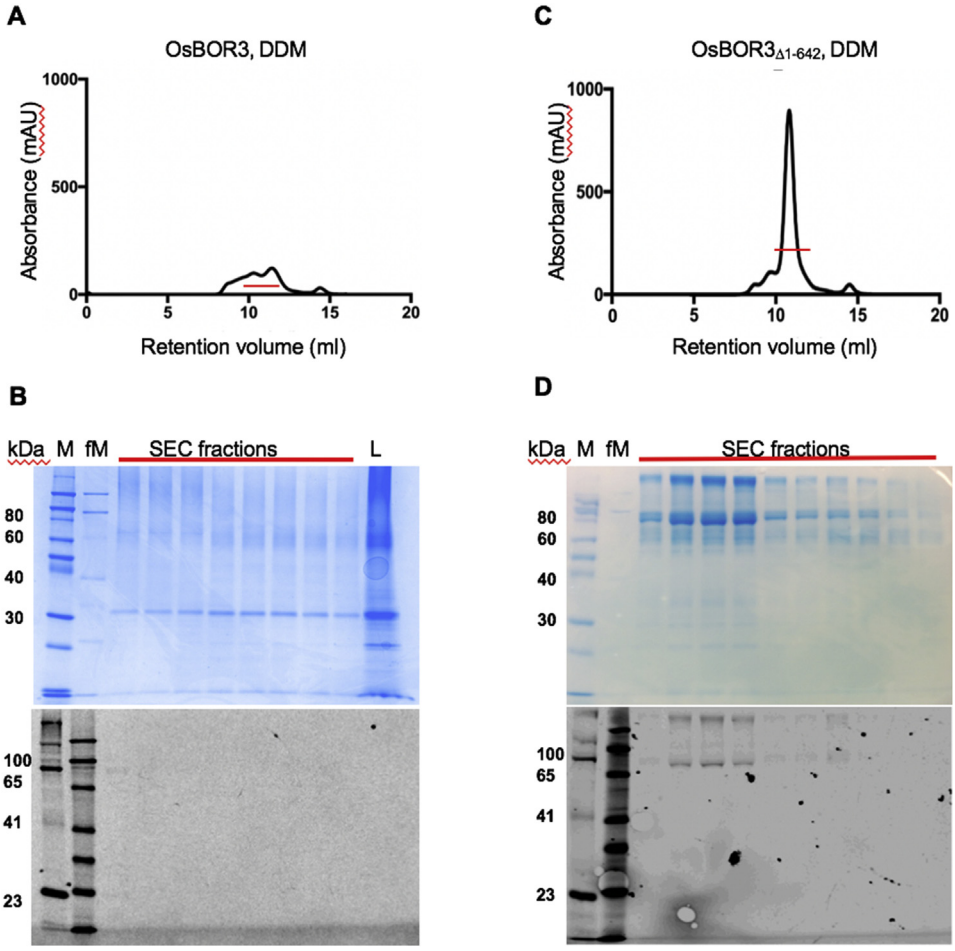

Fig. 1. Isolation of OsBOR3 proteins in DDM. Size exclusion profiles of A) WT OsBOR3 and C) $OsBOR3_{\Delta1\text{-}642}$ are shown. SDS-PAGE (upper panels) and in-gel fluorescence analysis (lower panels) for B) WT OsBOR3 and D) $OsBOR3_{\Delta1\text{-}642}$ are also shown. M = Molecular weight markers, fM = fluorescent molecular weight markers, L = concentrated protein solution loaded onto SEC column. The red lines indicate the SEC fractions that were analysed on SDS-PAGE. (For interpretation of the references to colour in this figure legend, the reader is referred to the Web version of this article.)

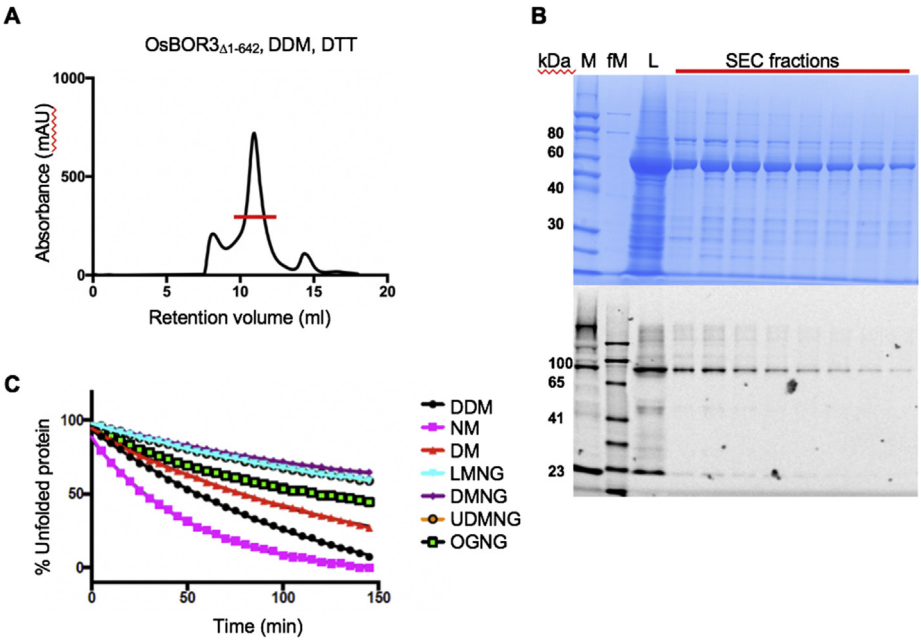

Fig. 2. Isolation of OsBOR3$_{\Delta 1\text{-}642}$ in DDM + DTT. Size exclusion profile A) and SDS-PAGE (upper panel) and in-gel fluorescence analysis (lower panels) B) are shown. M = Molecular weight markers, fM = fluorescent molecular weight markers, L = concentrated protein solution loaded onto SEC column. The red lines indicate the SEC fractions that were analysed on SDS-PAGE. C) Thermal denaturation analysis of OsBOR3$_{\Delta 1\text{-}642}$ in a range of detergents. The denaturation curves obtained in the individual detergents are indicated by the key. (For interpretation of the references to colour in this figure legend, the reader is referred to the Web version of this article.)

an artefact of the gel running process or genuine heterogeneity of the sample. In an effort to deal with any possible aggregation that might be occurring as the result of non-specific disulphide bridges (there are 7 cysteines in OsBOR3$_{\Delta 1\text{-}642}$) and contributing to heterogeneity, we attempted purification of the protein in the presence of 2 mM DTT. The SEC trace we obtained looked slightly worse than for DDM alone but a single prominent band of roughly 60 kDa is now apparent on the gel, although a weaker band of ~80 kDa is also visible (Fig. 2B, upper panel). In addition, the sample contains fluorescent protein which also migrates to ~80 kDa (Fig. 2B, lower panel). Thus, it is possible that the sample contains both OsBOR3$_{\Delta 1\text{-}642}$ that has effectively had the GFP cleaved (60 kDa) as well as uncleaved fusion protein (~80 kDa).

In order to improve the quality of the protein, we explored the use of other detergents using thermal denaturation analysis of the most promising construct, OsBOR3$_{\Delta 1\text{-}642}$, purified in DDM and then diluted in a range of alternative detergents. The CPM dye used becomes fluorescent upon binding to free Cys residues as they become available during protein unfolding. The data shown in Fig. 2C reveals that the protein was more stable in the MNGs tested, LMNG, UDMNG and DMNG compared to the alkyl maltosides (DDM, NM). As there was no discrimination between the three MNGs we chose initially to purify the OsBOR3$_{\Delta 1\text{-}642}$ in LMNG as it had been used successfully for isolation and crystallisation of AtBOR1 [29].

3.2. Isolation in LMNG

The OsBOR3$_{\Delta 1\text{-}642}$ was both extracted in (1%) and purified (0.01%) in LMNG. The LMNG extracted OsBOR3$_{\Delta 1\text{-}642}$ with a solubilisation efficiency of 80%. Isolation carried out as described above for DDM yielded a greater quantity of protein (0.125 vs 0.100 mg/L) which eluted from the SEC column as a single large peak at an elution volume of ~11 mls (Fig. 3A). SDS-PAGE and in-gel fluorescence analysis of the individual fractions revealed that the protein sample was both very heterogeneous and heavily contaminated with fluorescent material, most likely uncleaved or partially cleaved OsBOR3$_{\Delta 1\text{-}642}$-GFP protein (Fig. 3B). As for the protein isolated in DDM, following concentration through a MWCO filter the protein sample was visibly green. A prominent band of ~200 kDa which is notably fluorescent may correspond to an aggregated form of the uncleaved protein. The band at ~80 kDa may be OsBOR3$_{\Delta 1\text{-}642}$ with the GFP still attached as it is highly fluorescent. A band at ~60 kDa is possibly cleaved OsBOR3$_{\Delta 1\text{-}642}$. Isolation of the protein in LMNG + 2 mM DTT resulted in much less heterogeneity of the sample on the SDS-PAGE gel (Fig. 3C and D, upper panel) which two main bands (~60 kDa and ~80 kDa). We postulated that both proteins are OsBOR3$_{\Delta 1\text{-}642}$, one the monomer and one the dimer form. MS confirmed that both bands are OsBOR3$_{\Delta 1\text{-}642}$ but the larger band was contaminated with GFP. This is also clear from Fig. 3C and D. This wasn't always the case however (Fig. 3E and F) as on some occasions it was possible to isolate the protein in LMNG with little or no contamination with fluorescent protein. The reasons for this variability in the protein quality are unclear, as are the precise nature of the effects of DTT. However, given the fact that the presence of DTT facilitated interpretation of the gel images and it had no negative effect on the apparent protein quality we retained this in further purification experiments. Long term stability analysis (Fig. 3G) indicates that the LMNG isolated OsBOR3$_{\Delta 1\text{-}642}$ material was reasonably stable at 4 °C, but subject to degradation at 20 °C.

3.3. Isolation in DMNG

Ready availability of DMNG made this the next obvious choice of detergent. DMNG has similar stabilising effects on OsBOR3$_{\Delta 1\text{-}642}$ as LMNG as indicated by the thermal denaturation analysis and has been successfully used for high resolution structure determination of membrane proteins, including the human GABA$_A$ receptor [40]. Solubilisation efficiency in this detergent was 80%, identical to LMNG. The SEC profile of OsBOR3$_{\Delta 1\text{-}642}$ in DMNG revealed the presence of two peaks, a smaller peak at an elution volume of ~11 mls and a much larger peak at an elution volume of ~12.5 mls (Fig. 4A). SDS-PAGE analysis indicated that the protein from both peaks migrated identically as a ~60 kDa band (Fig. 4B, upper panel). Mass spectrometry analysis (data not shown) confirmed that the protein from both peaks was OsBOR3$_{\Delta 1\text{-}642}$. It seems likely that in DMNG the protein is present in two forms, likely the monomer (migrating at ~ 60 kDa on the SDS-PAGE gel and eluting at 12.5 mls from the SEC column) and the dimer (which migrates as the monomer form on the SDS-PAGE gel and elutes at 11 mls from the SEC column). The DMNG isolated protein is highly homogeneous and contains only very low levels of fluorescence (Fig. 4B, lower panel). Long term stability analysis indicated that the protein in the larger peak (probable monomer) is also highly stable, retaining almost full integrity over a four day incubation at 4 °C or 20 °C, as revealed by SDS-PAGE analysis (Fig. 4C).

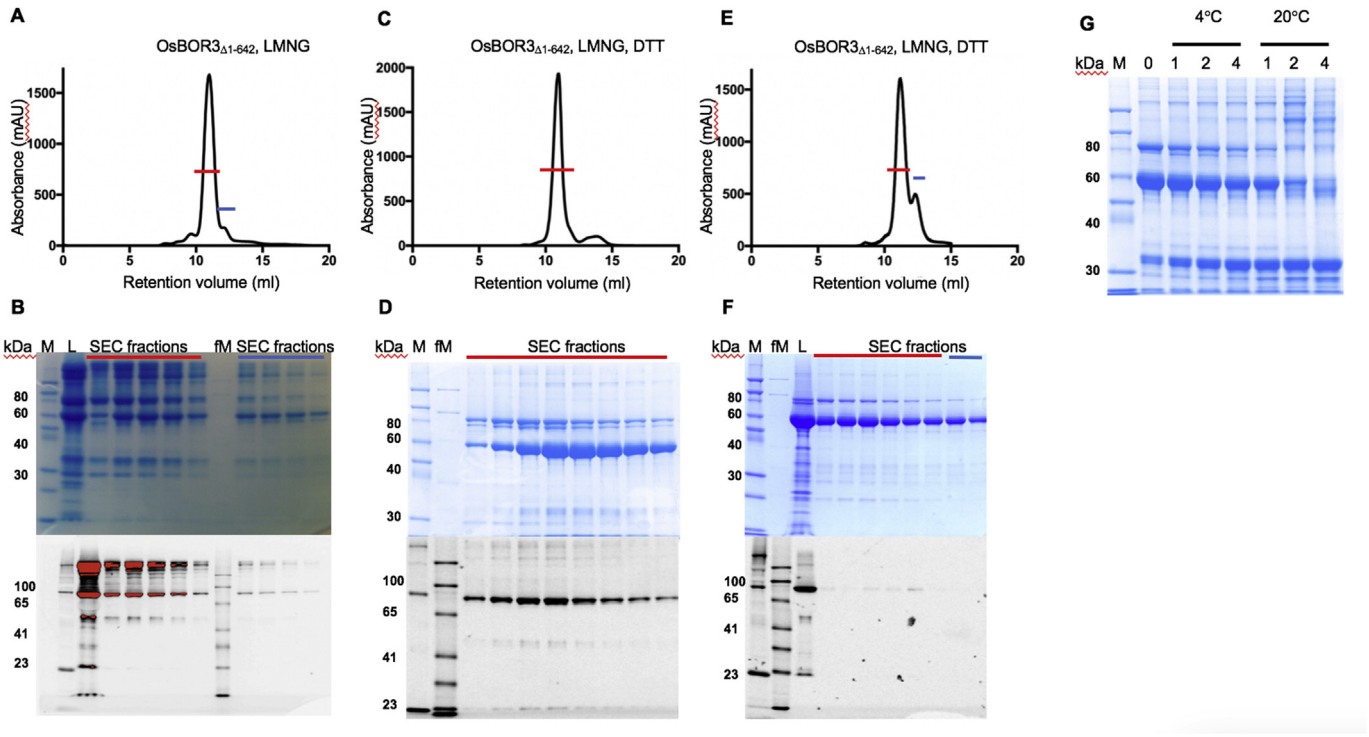

Fig. 3. Isolation of OsBOR3$_{\Delta 1\text{-}642}$ in LMNG. Size exclusion profiles of OsBOR3$_{\Delta 1\text{-}642}$ isolated in LMNG A) and LMNG + DTT C)+E) are shown. SDS-PAGE (upper panels) and in-gel fluorescence analysis (lower panels) for B) LMNG and D)+F) LMNG + DTT isolated protein are also shown. M = Molecular weight markers, fM = fluorescent molecular weight markers, L = concentrated protein solution loaded onto SEC column. The red and blue lines indicate the SEC fractions that were analysed on SDS-PAGE. G) Long term stability analysis of OsBOR3$_{\Delta 1\text{-}642}$ isolated in LMNG + DTT. Protein in Lane labelled as 0 is the protein analysed immediately after isolation, i.e. Day 0. The protein samples taken on subsequent days are indicated. (For interpretation of the references to colour in this figure legend, the reader is referred to the Web version of this article.)

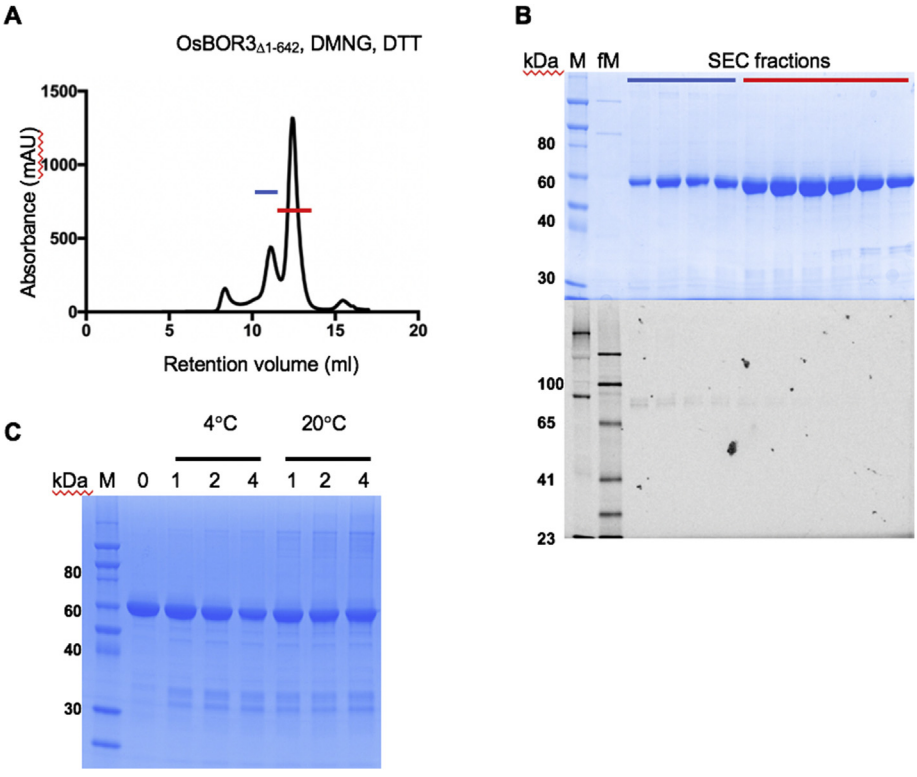

Fig. 4. Isolation of OsBOR3$_{\Delta 1\text{-}642}$ in DMNG + DTT. Size exclusion profile A) and SDS-PAGE (upper panel) and in-gel fluorescence analysis (lower panels) B) are shown. M = Molecular weight markers, fM = fluorescent molecular weight markers. The red and blue lines indicate the SEC fractions that were analysed on SDS-PAGE. Note the difference in retention volume of the DMNG isolated protein compared to that isolated in the other tested detergents. Long term stability analysis of OsBOR3$_{\Delta 1\text{-}642}$ isolated in LMNG + DTT. Protein in Lane labelled as 0 is the protein analysed immediately after isolation, i.e. Day 0. The protein samples taken on subsequent days are indicated. (For interpretation of the references to colour in this figure legend, the reader is referred to the Web version of this article.)

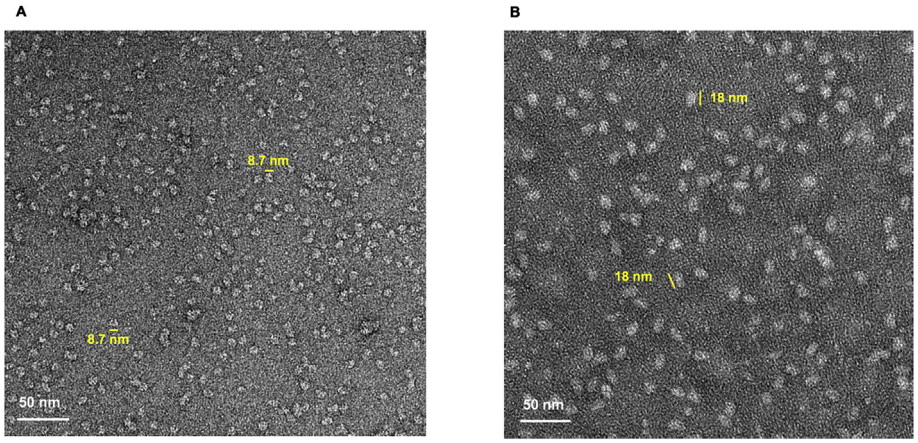

Fig. 5. Negative stain analysis of OsBOR3$_{\Delta 1\text{-}642}$. Negative stain images of protein isolated in LMNG A) and DMNG B) + DTT. The scale bar represents 50 nm.

3.4. Negative stain EM analysis

Negative stain of both LMNG and DMNG isolated OsBOR3$_{\Delta 1\text{-}642}$ was carried out (Fig. 5). Both proteins seem to be visible as single particles with the LMNG particles bigger than the DMNG ones, possibly reflecting a dimeric rather than a monomeric state of the protein. The DMNG images were of better quality than the LMNG although this could just require additional screening.

4. Discussion

Isolation of integral membrane proteins in their folded and correct quaternary state remains a challenge for structure determination. Protein engineering and development of novel detergents represent two ways to facilitate the isolation and stabilisation of membrane proteins [41]. Here we applied both approaches to the successful isolation of both monomeric and dimeric forms of OsBOR3.

The removal of what is likely to be a highly flexible extended C-terminal domain (the last 30 residues), as reported for the AtBOR1 protein [29], dramatically improved recovery of OsBOR3 protein in DDM in terms of both yield and quality of material. The full length OsBOR3 has 9 Cys whereas the truncated OsBOR3$_{\Delta 1\text{-}642}$ contains 7. The odd number of Cys might contribute to formation of non-specific disulphide bonds. Although, the SEC profiles changed little upon addition of DTT, the presence of this agent did make interpretation of the gel images easier. The actual effects of DTT remain unclear. However, the OsBOR3$_{\Delta 1\text{-}642}$ purified in the presence of DDM +/− DTT was contaminated with fluorescent protein strongly suggesting that GFP was not effectively cleaved from the transporter during isolation. It is possible this is the result of the DDM micelle shielding the TEV cleavage site given the closer proximity of the C-terminus of OsBOR3 in the truncated protein or that non-specific oligomerisation occurring as a result of the disulphide bridge formation limits access of the TEV enzyme. Contamination with fluorescent protein was sometimes also the case for isolation of OsBOR3$_{\Delta 1\text{-}642}$ in LMNG which also forms a large micelle.

Protein obtained in the slightly smaller micelle forming DMNG + DTT was not contaminated with fluorescent protein supporting the argument that it is the detergent which is limiting TEV cleavage. A further key difference was that the DMNG isolated protein eluted at a substantially higher retention volume. This taken together with 1) the almost identical SDS-PAGE results obtained for both DMNG and LMNG + DTT and, 2) MS analysis confirming that protein isolated in both detergents is OsBOR3$_{\Delta 1\text{-}642}$ strongly indicate that DMNG isolated protein is in a different oligomeric status. It is difficult to be confident from SDS-PAGE analysis precisely what species is present in an individual sample. Clearly oligomers are prone to dissociate into the monomeric form during electrophoresis and migration of individual membrane proteins is anomalous with membrane proteins typically appearing smaller than they are on the gel [38]. However, that protein isolated in DMNG and LMNG contains predominantly monomer and dimer is supported by the sizes of the particles obtained by negative stain electron microscopy in each case.

Given the similarity between OsBOR3 and other SLC4 proteins [29–31] as well as UapA [32] and UraA [33] it seems likely that the OsBOR3 dimer is physiologically relevant. Several of these proteins have been suggested to transport via an elevator mechanism requiring a substantial movement of approximately 10 Å of the substrate binding, or core, domain of a monomer against the dimerization, or gate, domain. It has been suggested that this radical structural movement is facilitated by the stabilising interactions formed between two monomers and possibly involving interactions with membrane lipids [42]. In the case of the BOR homologue from *S. cerevisiae*, ScBOR1p, we now have evidence that the protein can function as a monomer [43], although we can't rule out that the dimer plays a role in function. It is not clear which oligomeric states is the functional form of OsBOR3, a feature that is challenging to definitively decipher even if a high-resolution structure is available.

The related protein AtBOR1 was isolated successfully in LMNG [29], while the C-terminal transmembrane domain of human homologue AE1 was isolated initially in Octaethylene glycol monododecyl ether ($C_{12}E_8$) followed by complex formation with a Fab fragment and exchange into DM [30]. In both cases a structure of a dimer was determined but it remains to be seen if this represents the functional form of the proteins. The fact that OsBOR3 can successfully be isolated both in the dimeric and monomeric forms indicates that the dimer is not essential for stability and structural integrity of the individual monomers.

Acknowledgments

This project has received funding from the European Union's Horizon 2020 research and innovation programme, RAMP-ITN: Rationalising Membrane Protein Crystallisation Innovative Training Network, under the Marie Sklodowska-Curie grant agreement No 722687 (CC). This work was also supported by Biotechnology and Biological Sciences Research Council (BBSRC) grant BB/N016467/1 awarded to BB, AC and AJ.

Appendix A. Supplementary data

Supplementary data to this article can be found online at https://doi.org/10.1016/j.pep.2019.105522.

References

[1] R. Santos, O. Ursu, A. Gaulton, A.P. Bento, R.S. Donadi, C.G. Bologa, et al., A comprehensive map of molecular drug targets, Nat. Rev. Drug Discov. 16 (2016) 19–34, https://doi.org/10.1038/nrd.2016.230.

[2] W.A. Hendrickson, Atomic-level analysis of membrane-protein structure, Nat. Struct. Mol. Biol. 23 (2016) 464–467, https://doi.org/10.1038/nsmb.3215.

[3] A. Pandey, K. Shin, R.E. Patterson, X.-Q. Liu, J.K. Rainey, Current strategies for protein production and purification enabling membrane protein structural biology, Biochem. Cell Biol. 94 (2016) 507–527, https://doi.org/10.1139/bcb-2015-0143.

[4] A.M. Seddon, P. Curnow, P.J. Booth, Membrane proteins, lipids and detergents: not just a soap opera, Biochim. Biophys. Acta Biomembr. 1666 (2004) 105–117, https://doi.org/10.1016/j.bbamem.2004.04.011.

[5] R.M. Garavito, S. Ferguson-Miller, Detergents as tools in membrane biochemistry, J. Biol. Chem. 276 (2001) 32403–32406, https://doi.org/10.1074/jbc.R100031200.

[6] G.G. Privé, Detergents for the stabilization and crystallization of membrane proteins, Methods 41 (2007) 388–397, https://doi.org/10.1016/j.ymeth.2007.01.007.

[7] Artem Stetsenko, Guskov Albert, An overview of the top ten detergents used for membrane protein crystallization, Crystals 7 (2017) 197, https://doi.org/10.1002/elsc.201400187.

[8] J.L. Parker, S. Newstead, Current trends in α-helical membrane protein crystallization: an update, Protein Sci. 21 (2012) 1358–1365.

[9] A. Sadaf, K.H. Cho, B. Byrne, P.S. Chae, Amphipathic agents for membrane protein study, Methods Enzymol. 557 (2015) 57–94, https://doi.org/10.1016/bs.mie.2014.12.021.

[10] W.-X. Hong, K.A. Baker, K.A. Baker, X. Ma, X. Ma, R.C. Stevens, et al., Design, synthesis, and properties of branch-chained maltoside detergents for stabilization and crystallization of integral membrane proteins: human connexin 26, Langmuir 26 (2010) 8690–8696, https://doi.org/10.1021/la904893d.

[11] P.S. Chae, S.G.F. Rasmussen, R.R. Rana, K. Gotfryd, A.C. Kruse, A. Manglik, et al., A new class of amphiphiles bearing rigid hydrophobic groups for solubilization and stabilization of membrane proteins, Chemistry 18 (2012) 9485–9490, https://doi.org/10.1002/chem.201200069.

[12] K.-A. Nguyen, M. Peuchmaur, S. Magnard, R. Haudecoeur, C. Boyère, S. Mounien, et al., Glycosyl-substituted dicarboxylates as detergents for the extraction, overstabilization, and crystallization of membrane proteins, Angew. Chem. Int. Ed. 57 (2018) 2948–2952, https://doi.org/10.1021/jacs.6b11997.

[13] P.S. Chae, S.G.F. Rasmussen, R.R. Rana, K. Gotfryd, R. Chandra, M.A. Goren, et al., Maltose-neopentyl glycol (MNG) amphiphiles for solubilization, stabilization and crystallization of membrane proteins, Nat. Methods 7 (2010) 1003–1008, https://doi.org/10.1038/nmeth.1526.

[14] P.S. Chae, R.R. Rana, K. Gotfryd, S.G.F. Rasmussen, A.C. Kruse, K.H. Cho, et al., Glucose-neopentyl glycol (GNG) amphiphiles for membrane protein study, Chem. Commun. (Camb.). 49 (2013) 2287–2289, https://doi.org/10.1039/c2cc36844g.

[15] M. Das, Y. Du, J.S. Mortensen, M. Ramos, L. Ghani, H.J. Lee, et al., Trehalose-cored amphiphiles for membrane protein stabilization: importance of the detergent micelle size in GPCR stability, Org. Biomol. Chem. 17 (2019) 3249–3257, https://doi.org/10.1039/C8OB03153C.

[16] J.L. Popot, E.A. Berry, D. Charvolin, C. Creuzenet, C. Ebel, D.M. Engelman, et al., Amphipols: polymeric surfactants for membrane biology research, Cell. Mol. Life Sci. 60 (2003) 1559–1574, https://doi.org/10.1007/s00018-003-3169-6.

[17] M.L. Carlson, J.W. Young, Z. Zhao, L. Fabre, D. Jun, J. Li, et al., The Peptidisc, a simple method for stabilizing membrane proteins in detergent-free solution, Elife 7 (2018) 215, https://doi.org/10.7554/eLife.34085.

[18] S. Schoebel, W. Mi, A. Stein, S. Ovchinnikov, R. Pavlovicz, F. Dimaio, et al., Cryo-EM structure of the protein-conducting ERAD channel Hrd1 in complex with Hrd3, Nature 548 (2017) 352–355, https://doi.org/10.1038/nature23314.

[19] H. Ho, A. Miu, M.K. Alexander, N.K. Garcia, A. Oh, I. Zilberleyb, et al., Structural basis for dual-mode inhibition of the ABC transporter MsbA, Nature 557 (2018) 196–201, https://doi.org/10.1038/s41586-018-0083-5.

[20] I.G. Denisov, S.G. Sligar, Nanodiscs for structural and functional studies of membrane proteins, Nat. Struct. Mol. Biol. 23 (2016) 481–486, https://doi.org/10.1038/nsmb.3195.

[21] T.J. Knowles, R. Finka, R. Finka, C. Smith, C. Smith, Y.-P. Lin, et al., Membrane proteins solubilized intact in lipid containing nanoparticles bounded by styrene maleic acid copolymer, J. Am. Chem. Soc. 131 (2009) 7484–7485, https://doi.org/10.1021/ja810046q.

[22] S.C. Lee, T.J. Knowles, V.L.G. Postis, M. Jamshad, R.A. Parslow, Y.-P. Lin, et al., A method for detergent-free isolation of membrane proteins in their local lipid environment, Nat. Protoc. 11 (2016) 1149–1162, https://doi.org/10.1038/nprot.2016.070.

[23] A.J. Rothnie, Detergent-free membrane protein purification, Methods Mol. Biol. 1432 (2016) 261–267, https://doi.org/10.1007/978-1-4939-3637-3_16.

[24] N.L. Pollock, S.C. Lee, J.H. Patel, A.A. Gulamhussein, A.J. Rothnie, Biochim. Biophys. Acta Biomembr. 1860 (2018) 809–817, https://doi.org/10.1016/j.bbamem.2017.08.012.

[25] V.M. Shorrocks, The occurrence and correction of boron deficiency, Plant Soil 198 (1997) 121–148.

[26] M.A. O'Neill, S. Eberhard, P. Albersheim, A.G. Darvill, Requirement of borate cross-linking of cell wall rhamnogalacturonan II for Arabidopsis growth, Science 294 (2001) 846–849, https://doi.org/10.1126/science.1062319.

[27] J. Takano, K. Noguchi, M. Yasumori, M. Kobayashi, Z. Gajdos, K. MIWA, et al., Arabidopsis boron transporter for xylem loading, Nature 420 (2002) 337–340, https://doi.org/10.1038/nature01139.

[28] J. Takano, K. MIWA, L. Yuan, N. von Wirén, T. Fujiwara, Endocytosis and degradation of BOR1, a boron transporter of Arabidopsis thaliana, regulated by boron availability, Proc. Natl. Acad. Sci. U. S. A. 102 (2005) 12276–12281, https://doi.org/10.1073/pnas.0502060102.

[29] B.H. Thurtle-Schmidt, R.M. Stroud, Structure of Bor1 supports an elevator transport mechanism for SLC4 anion exchangers, Proc. Natl. Acad. Sci. U. S. A. 113 (2016) 10542–10546, https://doi.org/10.1073/pnas.1612603113.

[30] T. Arakawa, T. Kobayashi-Yurugi, Y. Alguel, H. Iwanari, H. Hatae, M. Iwata, et al., Crystal structure of the anion exchanger domain of human erythrocyte band 3, Science (New York, N.Y.) 350 (2015) 680–684, https://doi.org/10.1126/science.aaa4335.

[31] K.W. Huynh, J. Jiang, N. Abuladze, K. Tsirulnikov, L. Kao, X. Shao, et al., CryoEM structure of the human SLC4A4 sodium- coupled acid-base transporter NBCe1, Nat. Commun. (2018) 1–9, https://doi.org/10.1038/s41467-018-03271-3.

[32] Y. Alguel, S. Amillis, J. Leung, G. Lambrinidis, S. Capaldi, N.J. Scull, et al., Structure of eukaryotic purine/H(+) symporter UapA suggests a role for homodimerization in transport activity, Nat. Commun. 7 (2016) 11336, https://doi.org/10.1038/ncomms11336.

[33] X. Yu, G. Yang, C. Yan, J.L. Baylon, J. Jiang, H. Fan, et al., Dimeric structure of the uracil:proton symporter UraA provides mechanistic insights into the SLC4/23/26 transporters, Cell Res. 27 (2017) 1020–1033, https://doi.org/10.1038/cr.2017.83.

[34] J. Kota, C.F. Gilstring, P.O. Ljungdahl, Membrane chaperone Shr3 assists in folding amino acid permeases preventing precocious ERAD, J. Cell Biol. 176 (2007) 617–628, https://doi.org/10.1083/jcb.200612100.

[35] J. Leung, A.D. Cameron, G. Diallinas, B. Byrne, Stabilizing the heterologously expressed uric acid-xanthine transporter UapA from the lower eukaryote Aspergillus nidulans, Mol. Membr. Biol. 30 (2013) 32–42, https://doi.org/10.3109/09687688.2012.690572.

[36] S. Newstead, H. Kim, G. von Heijne, S. Iwata, D. Drew, High-throughput fluorescent-based optimization of eukaryotic membrane protein overexpression and purification in Saccharomyces cerevisiae, Proc. Natl. Acad. Sci. 104 (2007) 13936–13941, https://doi.org/10.1073/pnas.0704546104.

[37] D. Drew, S. Newstead, Y. Sonoda, Y. Sonoda, H. Kim, H. Kim, et al., GFP-based optimization scheme for the overexpression and purification of eukaryotic membrane proteins in Saccharomyces cerevisiae, Nat. Protoc. 3 (2008) 784–798, https://doi.org/10.1038/nprot.2008.44.

[38] A. Rath, M. Glibowicka, V.G. Nadeau, G. Chen, C.M. Deber, Detergent binding explains anomalous SDS-PAGE migration of membrane proteins, Proc. Natl. Acad. Sci. U. S. A. 106 (2009) 1760–1765, https://doi.org/10.1073/pnas.0813167106.

[39] N. Coudray, S. L Seyler, R. Lasala, Z. Zhang, K.M. Clark, M.E. Dumont, et al., Structure of the SLC4 transporter Bor1p in an inward-facing conformation, Protein Sci. 26 (2017) 130–145, https://doi.org/10.1002/pro.3061.

[40] P.S. Miller, A.R. Aricescu, Crystal structure of a human GABAA receptor, Nature 512 (2014) 270–275, https://doi.org/10.1073/pnas.0810590106.

[41] N. Bertheleme, P.S. Chae, S. Singh, D. Mossakowska, M.M. Hann, K.J. Smith, et al., Unlocking the secrets of the gatekeeper: methods for stabilizing and crystallizing GPCRs, Biochim. Biophys. Acta 1828 (2013) 2583–2591, https://doi.org/10.1016/j.bbamem.2013.07.013.

[42] E. Pyle, A.C. Kalli, S. Amillis, Z. Hall, A.M. Lau, A.C. Hanyaloglu, et al., Structural lipids enable the formation of functional oligomers of the eukaryotic purine symporter UapA, Cell Chem. Biol. 25 (2018) 840–848, https://doi.org/10.1016/j.chembiol.2018.03.011 e4.

[43] E. Pyle, C. Guo, T. Hofmann, C. Schmidt, O. Ribeiro, A. Politis, et al., Protein-lipid interactions stabilise the oligomeric state of Bor1p from Saccharomyces cerevisiae, Anal. Chem. (2019), https://doi.org/10.1021/acs.analchem.9b03271 acs.analchem.9b03271.